WATER RESOURCES RESEARCH, VOL. 45, W08407, doi:10.1029/2008WR007230, 2009

Ecohydrological optimization of pattern and processes in water-limited ecosystems: A trade-off-based hypothesis

Kelly K. Caylor,[1] Todd M. Scanlon,[2] and Ignacio Rodriguez-Iturbe[1]

Received 18 June 2008; revised 8 May 2009; accepted 26 May 2009; published 7 August 2009.

[1] The complex interactions between plants, soils, and climates in semiarid ecosystems make it difficult to define specific ecohydrological optimization mechanisms that underlie observed spatiotemporal patterns of vegetation structure. There remains a clear need to develop conceptual models that are capable of interpreting and predicting spatial pattern formation in savannas (and similar dry woodland ecosystems), as well as metrics for assessing optimization or organization of patterns, as one scales from individual canopies to landscapes and beyond. In this article, we propose a unifying hypothesis regarding ecohydrological optimization of pattern and processes, namely, that vegetation patterns in water-limited environments are constrained in their ability to maximize water use by a need to simultaneously minimize water stress. We use this trade-off-based hypothesis to infer the function of dryland ecosystems under a wide range of scales and applications. Specifically, we examine spatial and temporal aspects of ecohydrological organization of vegetation patterns for three different cases: (1) patterns of regional-scale temporal organization across a regional climate gradient, (2) patterns of landscape-scale spatial organization within a semiarid drainage basin, and (3) patterns of individual-scale structural organization across varying soil textures. Although the insight gained from each of these examples is derived from specific modeling approaches, each of which contains its own unique set of assumptions and limitations, they are unified by our proposed ecohydrological trade-off approach that simultaneously considers both plant water deficit and plant water use as a diagnostic tool for assessing vegetation patterns in water-limited environments. It is our hope that the ongoing development of coupled ecological and hydrological models capable of assessing a diversity of interactions between plants, soils, and climates will lead to the emergence of more generalized hypotheses regarding the manner by which ecological and hydrological patterns coorganize in landscapes.

Citation: Caylor, K. K., T. M. Scanlon, and I. Rodriguez-Iturbe (2009), Ecohydrological optimization of pattern and processes in water-limited ecosystems: A trade-off-based hypothesis, *Water Resour. Res.*, *45*, W08407, doi:10.1029/2008WR007230.

1. Introduction

[2] Clarification of the coupled ecological and hydrological mechanisms that determine vegetation structure and function remains a vexing problem in both hydrological and vegetation science [*Newman et al.*, 2006]. The coupled nature of hydrological and ecological dynamics is perhaps nowhere more evident than in semiarid ecosystems. Frequently stressed and sensitive to change [*Guenther et al.*, 1996], semiarid ecosystems are responsive to climate variability over relatively short time scales, and water is a main driving force in shaping the vegetation distribution and composition [*Rodriguez-Iturbe et al.*, 1999a; *Smit and Rethman*, 2000]. The dynamical nature of the vegetation response to water availability is a prominent feature of semiarid ecosystem function, as is evident from satellite observations [*Goward and Prince*, 1995; *Scanlon et al.*, 2002]. The strength and importance of couplings between ecological and hydrological dynamics has led to the emergence of ecohydrology as a multidisciplinary research topic [*Bond*, 2003; *Hannah et al.*, 2004; *Edreny*, 2005; *Breshears*, 2005]. Despite the close coupling that exists between water and vegetation structure, the challenge of predicting vegetation response to changing climate in these environments is particularly daunting [*Daly et al.*, 2000]. Specifically, a central challenge is defining the ecologically and hydrologically relevant processes that lead to the formation of vegetation patterns in water-limited ecosystems [*Sole*, 2007].

[3] The complex interactions between plants, soils, and climates in semiarid ecosystems make it difficult to define specific ecohydrological optimization mechanisms that underlie observed landscape-scale patterns in vegetation structure. Regional models of semiarid vegetation structure are often biogeographical in nature, making predictions based exclusively on the role of external factors such as mean annual rainfall, or soil infertility imposed by geologic

---

[1] Department of Civil and Environmental Engineering, Princeton University, Princeton, New Jersey, USA.

[2] Department of Environmental Sciences, University of Virginia, Charlottesville, Virginia, USA.

0043-1397/09/2008WR007230$09.00

constraints. These kinds of relationships often yield reasonable predictions of savanna ecosystem structure [*Sankaran et al.*, 2005; *Huxman et al.*, 2005], but provide little additional insight in the specific ecohydrological processes that maintain vegetation-climate coorganization. Indeed, the strong control that individual plants can exert on local water balance has been highlighted by the field observations of *Seyfried et al.* [2005] and *Ludwig et al.* [2005] who demonstrate variation in surface moisture redistribution caused by the mosaic of vegetation patches and interpatch areas in a variety of semiarid ecosystems. The conceptual models arising from these field-scale studies explicitly couple biological pattern to abiotic factors; usually driven by soil moisture, but often also thought to be determined by nutrients, herbivory, or fire. On the basis of these considerations, more recent models of savanna structure have taken the small-scale spatial structure of semiarid ecosystems into account [*Jeltsch et al.*, 1999; *Scanlon et al.*, 2007].

[4] Theoretical treatments of coupled plant-soil-climate determinants of soil moisture dynamics [*Feddes et al.*, 1988; *Rodriguez-Iturbe et al.*, 1999b; *Laio et al.*, 2001b; *Albertson and Montaldo*, 2003] have suggested a number of general principles that may guide the coorganization of biological communities and hydrological dynamics in dryland environments. Perhaps the best known optimality theory is that proposed by *Eagleson and Segarra* [1985], which defined optimal hydrological conditions for ecosystem function as minimization of canopy stress and maximization of soil moisture. While intuitively reasonable [*Hatton et al.*, 1997], the justification of these premises from an ecological perspective appears to be questionable [*Kerkhoff et al.*, 2004]. Other approaches focus only on aboveground optimization of plant form [*Eagleson*, 2002], neglect the spatial complexity of dryland vegetation [*Porporato et al.*, 2001], or greatly simplify soil moisture dynamics [*Schwinning and Ehleringer*, 2001].

[5] There remains a need to clarify the manner by which vegetation self-organizes across scales within semiarid landscapes and how regional-, landscape-, and individual-based patterns of vegetation interact with their accompanying climates and soils. Such clarification necessitates the development of conceptual models capable of interpreting and predicting spatial pattern formation in savannas (and similar dry woodland ecosystems) as well as metrics for assessing optimization or organization of patterns as one scales from individual canopies to landscapes and beyond. In our view, a key difficulty arises in developing metrics of optimization that are relevant across a range of different spatial and temporal scales of interest.

[6] In general, hydrological theories of dryland function can be broadly grouped into two categories. The first treats maximization of water use (episodic growth) as the primary organizing principle, while the second treats minimization of water stress (episodic drought) as the most critical factor governing vegetation dynamics. Clearly both factors act to determine the dynamics of dryland ecosystems in space and time. Examples of changes in relative growth rates leading to shifts in ecosystem structure include bush encroachment [*Huxman et al.*, 2005; *Brown and Archer*, 1999] and the historical expansion of invasive species [*Bond et al.*, 2003] in many dry lands. In contrast, recent droughts in the desert southwest of the US [*Breshears et al.*, 2005] have demonstrated the enormous potential for periods of chronic resource scarcity to rapidly transform ecosystem structure. While specific examples may appear to present contradictory evidence for the mechanisms that control dryland ecosystem structure, our goal is the articulation of more general principles that operate to govern the dynamic feedbacks between vegetation and resource availability across a variety climates and ecosystems.

[7] To this end, we present here an exploration of a general hypothesis that the spatiotemporal organization of semiarid ecosystems can be best described through the consideration of an explicit trade-off between resource use (growth) and stress avoidance (survival). While some of the methods and approaches contained in this manuscript have been presented elsewhere by the authors in a variety of venues [*Scanlon et al.*, 2005; *Caylor et al.*, 2004b, 2005, 2006], we seek to unify these similar but distinct prior efforts in order to characterize dryland vegetation organization through a common hypothesis. Specifically, we have revisited our past approaches in order to examine the utility of the above unifying hypothesis as a means of explaining dryland ecohydrological organization across a wide range of scales and applications.

[8] In the current discussion we focus on the spatial and temporal aspects of interactions between plants, soils, and climates in a variety of different water-limited systems. Our examples are drawn from a series of savanna sites spanning a large rainfall gradient within southern Africa, as well as from a semiarid river basin organized around an ephemeral drainage network in central New Mexico. We address our hypotheses regarding coorganization of patterns and processes around resource trade-offs at a hierarchy of scales that range from climate gradients spanning thousands of kilometers to individual tree canopies spanning only a few meters.

2. Temporal Signatures of Ecohydrological Optimization Within Semiarid Regions

[9] Satellite observations have revealed that transitional zones between woodland and desert ecosystems are hot spots of interannual variability in Normalized Difference Vegetation Index (NDVI) [*Goward and Prince*, 1995; *Williams and Albertson*, 2005]. The high variability in NDVI has been attributed to the dynamical aspect of vegetation in these typically water limited regions where vegetation biomass resonates with wet season rainfall. In seeking to define the coupling between hydrological and ecological processes, this prominent feature of water-limited ecosystems cannot be overlooked. Here we examine the role of the dynamic vegetation in mediating the hydrological cycle at the land surface and explore the significance of the dynamic vegetation on ecosystem function.

[10] The setting of the regional analysis is the Kalahari Transect (KT) in southern Africa, where grass cover is the primary dynamical component of the savanna vegetation. The Kalahari Transect is one of a number of International-Geosphere-Biosphere Programme (IGBP) transects designated throughout the world [*Koch et al.*, 1995] and covers a latitudinal mean annual rainfall gradient varying from approximately 1000 mm a^{-1} in the north to 250 mm a^{-1} in the south. Consistency in geomorphology and homogeneous soil conditions over the entire region, primarily deep

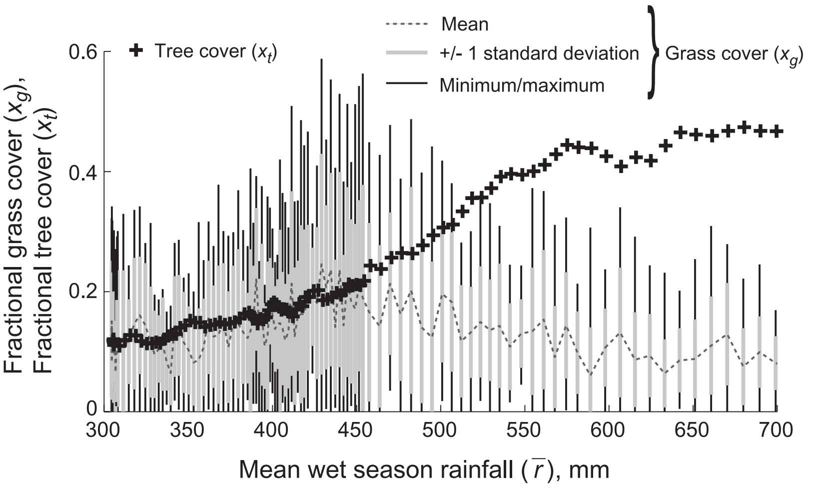

Figure 1. Distribution of fractional tree cover (x_t, crosses) and fractional grass cover (x_g, dashed line) with respect to mean wet season rainfall ($\bar{r}$) along the water-limited portion of the Kalahari Transect, derived from satellite data by the method of *Scanlon et al.* [2002]. Fractional tree cover has a strong linear relationship with mean rainfall ($R^2 = 0.94$); while fractional grass cover peaks near the middle of the transect (~450 mm wet season rainfall). Bars indicate the range (black bars) and standard deviation (gray bars) of the dynamic fractional grass cover for the 1983–1998 wet seasons.

Kalahari sands [*Thomas and Shaw*, 1991], allows for an analysis of vegetation structure and ecosystem processes relatively independent of soil type. Another amenable aspect for regional analysis is the low human population density of the Kalahari, which reduces anthropogenic impact on land cover. The gradient in mean annual rainfall across the Kalahari Transect sites results in dramatic variation in vegetation structure along the transect, which has been well characterized by ground-based measurements [*Caylor et al.*, 2004a; *Privette et al.*, 2004; *Scholes et al.*, 2002].

[11] Functional classes of woody versus grass vegetation exhibit disparate responses to interannual variability in wet season rainfall, owing to their specific structure and water use characteristics. Woody vegetation generally have extensive root systems, growth constrained by the existing woody structure, and lower water use efficiencies associated with C_3 plants, while Kalahari grasses have intensive root systems, a large potential for lateral growth, and relatively higher water use efficiencies as C_4 plants. *Scanlon et al.* [2002] examined the varying responses of trees and grasses to water availability and developed an unmixing algorithm based on the individual sensitivities of tree, grass, and bare soil NDVI to fluctuations in wet season rainfall to define their respective fractional covers along the KT. When the unmixing results were combined with a Soil-Vegetation-Atmosphere Transfer (SVAT) model [*Scanlon and Albertson*, 2003], the water-limited portion of the transect was found to be confined to the region where mean wet season rainfall was less than approximately 700 mm. Some combination of either nutrients or light are presumed to be limiting for portions of the KT that receive greater than this amount of mean wet season rainfall. The model-derived threshold corresponds to the geographical location along the transect where vegetation transitions from nutrient-rich, broad-leaved to nutrient-poor, fine-leaved savanna [*Scholes and Walker*, 1993], an independent confirmation of the SVAT model results.

[12] Mean wet season rainfall ($\bar{r}$) explains a large portion of the variance in tree fractional cover (x_t) along the water-limited portion of the transect ($R^2 = 0.94$) (Figure 1). The fractional grass cover (x_g), which is dynamic and driven by the amount of wet season rainfall received in a given year, exhibits a more complex pattern. Both the mean and variance in the extent of the grass cover peak at a mean wet season rainfall of approximately 450 mm. Rainfall limits the extent of the grass cover below this value, while the greater presence of trees in the wetter portion of the transect imposes a light limitation on grass growth above 450 mm. The satellite-derived fractional covers along the KT provide a starting point for understanding how these vegetation components interact with the land surface hydrological cycle.

2.1. A Regional-Scale SVAT Model With Dynamic Vegetation

[13] As a natural extension of earlier analytical work that assumed static rainfall and vegetation [*Eagleson and Segarra*, 1985; *Eagleson*, 1978], and variable rainfall and static vegetation [*Laio et al.*, 2001a; *Porporato et al.*, 2001; *Rodriguez-Iturbe et al.*, 2001], *Scanlon et al.* [2005] presented a modeling framework for the dynamical simulation of both rainfall and vegetation. This approach allowed for the evaluation of the ecohydrological role of observed grass dynamics with respect to regional water use and the occurrence of plant water stress. The SVAT modeling scheme was built upon the mathematical framework of *Scanlon and Albertson* [2003] by allowing the fraction of grass cover, x_g, to evolve throughout each wet season according to a growth/decay equation governed by the soil moisture in the near-surface soil layer. Temporal dynamics of x_g were simulated by the simple equation

$$\frac{dx_g}{dt} = ET_g\chi(1 - x_t) - \xi_g\eta x_g, \qquad (1)$$

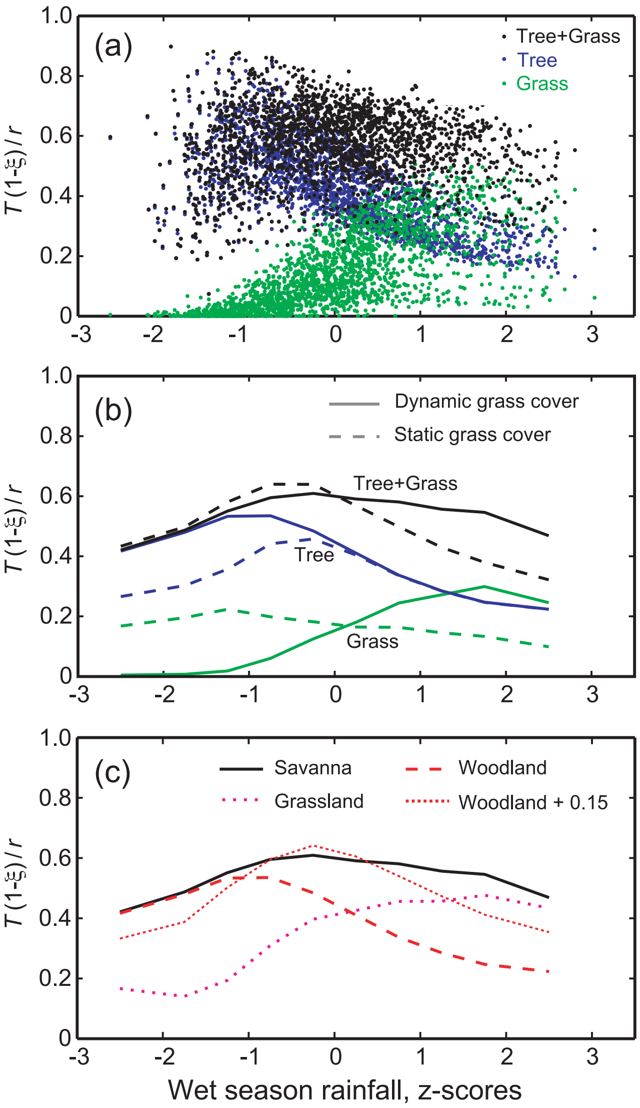

Figure 2. Results of the SVAT model applied over 16 wet seasons at 127 locations along the Kalahari Transect (KT). (a) Individual results of stress-weighted plant water uptake normalized by wet season rainfall, $T(1 - \xi)/r$, are plotted as a function of the z scores of wet season rainfall for the tree, grass, and combined cover for the observed savanna vegetation. (b) Mean wet season responses for the original model and a model run with a static grass cover in which x_g along the KT was set to its mean value. (c) Mean responses for the observed savanna vegetation and those for grassland, woodland, and woodland with fractional tree cover increased by 0.15 throughout the region. The broad peak of $T(1 - \xi)/r$ over the range of variability in wet season rainfall implies greater fitness of the savanna ecosystem with respect to optimal water use.

where ET_g represents transpiration by grasses, χ is a water use efficiency parameter, x_t is fractional tree cover, and η is a coefficient of grass mortality associated with the occurrence of grass water stress ξ_g. *Porporato et al.* [2001] review the physiological impacts of reduced water variability on plant performance, the onset of plant water stress, and the manner by which these complex phenomena can be incorporated into models of surface water balance. Here we adopt the water stress formulation first proposed by *Rodriguez-Iturbe et al.* [1999a], which determines the relative degree of plant water stress, ξ (dimensionless, varying between 0 and 1), according to the frequency and magnitude of excursions of the relative soil moisture below the critical value of s^* that corresponds to the point at which plants begin to close their stomata. At values of soil moisture above this critical value, plant stress is zero, while it becomes 1 when the soil moisture saturation is equal to or less than the plant wilting point (s_w). The general equation for this form of the plant water stress function is given by

$$\xi(s) = \begin{cases} 1 & s \leq s_w \\ \left(\dfrac{s^* - s}{s^* - s_w}\right)^q & s_w < s \leq s^*, \\ 0 & s > s^* \end{cases} \tag{2}$$

where q is a measure of nonlinearity in the relationship between relative soil moisture deficit and plant stress response, here taken to be equal to 2 following the discussion by *Porporato et al.* [2001].

[14] Calibration was necessary only for χ and η, which were adjusted to match the model output with the satellite observations. All of the other SVAT model inputs and parameters were taken from satellite data, best estimates from field data, or ground-based eddy covariance measurements for a series of sites along the KT [*Scanlon and Albertson*, 2004]. As shown by *Scanlon et al.* [2005], this simple equation was successful in capturing the mean and variability in satellite-observed grass cover along the Kalahari Transect.

[15] The daily SVAT model was applied over a time frame of 16 wet seasons (1983–1998) along the portion of the Kalahari Transect that receives less than 700 mm of mean wet season rainfall. We now proceed to evaluate ecosystem water use for this regional setting where interannual variability in rainfall supplies a fluctuating limiting resource. We do this by considering two quantities, the seasonal average rate of transpiration (T), and the seasonal average value of water stress (ξ), which are combined to yield what we call "stress-weighted plant water uptake" (ζ) following the general form

$$\zeta = T(1 - \xi), \tag{3}$$

which is used throughout the present paper. We hypothesize that maximization of water use and minimization of water stress, as captured by this single metric, is fundamental to the spatial organization of water-limited vegetation across multiple scales. Applied across the regional rainfall gradient, this function is normalized by wet season rainfall, r, and ξ is taken as the average water stress throughout the season. Fluctuations in wet season rainfall are described by their z scores, $(r - \bar{r})/\sigma_r$, where r is wet season rainfall in a given year, and σ_r is the standard deviation of wet season rainfall at a particular location.

[16] Model results for a 16-year simulation applied to 127 positions along the rainfall gradient are shown in Figure 2a. Components of $T(1 - \xi)/r$ for the tree and grass cover are plotted along with their sum, which describes the overall

$T(1 - \xi)/r$ for the savanna ecosystem. During dry years, grass cover is water stressed and limited in extent, whereas favorable conditions for growth that arise during wet years generally lead to higher grass-specific $T(1 - \xi)/r$. Trees tend to be more efficient in terms of their use of available water during dry years when grass fractional cover is suppressed. During wet years, factors such as increased grass transpiration and leakage loss from the root zone account for greater portions of the surface water balance. Although there is considerable scatter in the combined $T(1 - \xi)/r$ for the trees and grasses, the nature of their individual behavior in response to rainfall leads to this quantity being remarkably level over the range in wet season rainfall variability. The general forms of these relationships are evident from Figure 2a even though these normalized results have been compiled from across a large gradient in mean wet season rainfall and vegetation cover (Figure 1).

[17] The role of the dynamic grass cover is evaluated by comparing the original model results with those obtained using static grass cover, in which x_g was set to its mean value at each location along the KT. Model results show that during dry years, the reduced extent of the dynamic grass cover has the effect of enhancing the stress-weighted water use for trees (Figure 2b). For wet years, the greater amount of water removed from the upper soil layers by the dynamic grass cover does not appear to significantly influence the tree water use, but it does lead to an increase in the overall ecosystem $T(1 - \xi)/r$. As pointed out by *Scanlon et al.* [2005], the dynamical nature of the grass cover helps close the tenuous water balance at the land surface by resonating with the high-frequency (i.e., subannual to annual) variability in rainfall. In terms of the summed $T(1 - \xi)/r$ for trees and grasses, the broad peak with respect to interannual rainfall variability (Figure 2b) implies ecosystem fitness in this water-limited environment, which is promoted by the dynamical nature of the grass cover.

[18] Seasonal rainfall with pronounced interannual variability is typical of savanna ecosystems [*Rodriguez-Iturbe and Porporato*, 2004]. We contend that the stochastic nature of this limiting resource, together with soil properties, are paramount in shaping the structural composition of the vegetation. From a water use perspective, a pure grassland or a pure woodland situated in the Kalahari would be less efficient than the existing mixed tree/grass savanna in terms of exploiting this limiting resource. We evaluate $T(1 - \zeta)/r$ with respect to normalized rainfall for a grassland ecosystem by removing tree cover from the model and allowing grass to grow unimpeded by x_t, according to equation (1). Consistently lower $T(1 - \zeta)/r$ is observed for the grassland ecosystem (Figure 2c). During wet years, this can be explained by the shallow root system of grasses, combined with the sandy soils and the exponential distribution of storm rainfall depths, which allows significant amounts of water to bypass the root zone of grassland vegetation. Although the absence of trees allows the grass biomass to be extraordinarily responsive to the rainfall, this does not make up for the decreased efficiency in water use imposed by the uniformly shallow root depth. During dry years, the limited extent of the grass cover prevents optimal use of water when it becomes available, and bare soil evaporation losses are considerable.

[19] In the case of woodland ecosystems, plant water use dynamics are constrained by the woody structure, thereby making this vegetation less adaptable to fluctuations in wet season rainfall. By preserving the observed tree cover along the KT and by eliminating grass cover, we find that $T(1 - \xi)/r$ for this woodland ecosystem would be similar to the savanna for dry years, but would be significantly less during wet years because of the lack of a dynamical vegetation component that could make optimal use of this increased water availability (Figure 2c). A more realistic conversion from savanna to woodland would involve an increase in fractional tree cover throughout the KT, which we roughly account for in the model by increasing x_t by 0.15. The results indicate that $T(1 - \xi)/r$ is on par with that for the savanna vegetation during average rainfall years, but the woodland experiences greater stress during dry years and cannot make full use of the rainfall in terms of converting it into transpiration during wet years (Figure 2c). Savanna vegetation is clearly superior to both grasslands and woodlands with respect to maximizing $T(1 - \xi)/r$ over the full range of fluctuating rainfall. We contend that the tree/grass mixture of a savanna ecosystem is an example of increased ecosystem robustness arising from the complex adaptive nature of vegetation assemblages [*Levin*, 1999].

2.2. A Regional Theory of Dynamic Stability Through Optimization of Water Use

[20] The overarching control of hydrological factors on savanna vegetation structure across the Kalahari Transect is apparent from the substantial correlation between mean wet season rainfall and tree fractional cover derived from satellite data [*Scanlon et al.*, 2002] and field measurements [*Scholes et al.*, 2002]. This is consistent with the meta-analysis by *Sankaran et al.* [2005] of African savanna ecosystems, where the maximum landscape-scale woody cover was found to be well correlated to mean annual rainfall at locations receiving less than 650 ±134 mm. These savanna ecosystems were considered by *Sankaran et al.* [2005] to be stable in the sense that mean rainfall controls tree cover and permits grass cover, while disturbance factors (e.g., fire and herbivory) provide an additional impact on the possible stable state. We agree with this general framework and elaborate on this by showing that dynamic grass cover, a significant feature of savanna ecosystems, promotes ecosystem stability through optimal use of a fluctuating limiting resource. We note that our conceptual model is counter to existing theories that assume savannas are dynamically unstable, and predict that vegetation would tend toward states of minimal structural diversity such as grasslands or woodlands in the absence of disturbance factors [e.g., *Jeltsch et al.*, 2000]. In contrast we find that, from an ecohydrological perspective, a homogeneous vegetation composition is inferior to a heterogeneous, functionally diverse savanna over the full range of rainfall variability encountered in this water-limited setting.

[21] The model results for this largely undisturbed and topographically uniform Kalahari Transect savanna system reveal the degree to which the present vegetation structure appears to be optimized with regard to water use. We note that the use of a two-layer scheme for modeling regional tree/grass water use neglects the potential for horizontal variability in soil moisture and the impacts of such vari-

ability on vegetation dynamics. However, more complicated landscapes may require a more nuanced view of spatial heterogeneity. Section 3 presents an approach for addressing the crucial role that regional topography plays in organizing the coupled patterns of climates, soils, and vegetation.

3. Spatial Signatures of Ecohydrological Optimization Within Semiarid Landscapes

[22] Topographically complex landscapes containing river basins represent a physical template of water availability that arises from at least three discrete aspects of environmental dynamics: (1) differential water inputs that arise from elevational precipitation gradients; (2) shifts in atmospheric water demand driven by climatological differences across the basin; and (3) emergent patterns of landscape soil moisture that are mediated by interactions between the distribution of vegetation, soils, and climate. All three of these factors interact to determine characteristic patterns of ecosystem water use and water stress, which have unique spatial signatures across any specific drainage basin. Therefore, across gradients of elevation we may expect increases in rainfall and reductions in potential evapotranspiration (lower temperatures), which may lead to patterns of increasing water availability in areas more distant from the basin outlet. In contrast, the patterns of water stress would be the opposite, with less soil water available closer to the basin outlet because of both lower rainfall and higher amounts of potential evapotranspiration. Because riparian zones in many semiarid regions are quite small, a common overall effect of these environmental patterns is that there are opposing gradients of water use and water stress as one moves through the basin's topographic profiles. In this section, we revisit an earlier analysis [*Caylor et al.*, 2004b, 2005] and examine the hypothesis that vegetation patterns arising in water-limited landscapes result from a trade-off condition that balances both resource consumption and stress avoidance, which is the same general organizing principle we adopted in section 2. Here we use this hypothesis to address the coorganization between ecological, hydrological, and geomorphological patterns in semiarid river basins.

[23] In a series of papers, *Caylor et al.* [2004b, 2005] analyzed and simulated the spatial distribution of water stress arising from different vegetation configurations in the Upper Rio Salado basin, located near the Sevilleta Long-term Ecological Research (LTER) site in central New Mexico. Using available geospatial data, soil, climate, and vegetation properties were assigned across the basin. The resulting probabilistic characteristics of steady state soil moisture distribution were analyzed along with the distribution of observed vegetation patterns, simulated vegetation dynamic water stress, and hydrological fluxes such as transpiration.

[24] As in section 2, we are interested in the manner by which vegetation patterns can be explained through consideration of the trade-offs between plant water use and plant water stress. In order to examine these processes within the Rio Salado basin, we have reanalyzed the basin using a new set of metrics consistent with those in section 2 on regional dynamics of vegetation within the Kalahari region of southern Africa. Specifically, we use the same measure of plant water use (T/r) and a slightly modified version of the static water stress (ξ'), which scales the statistical steady state stress condition according to the duration of the mean first passage time between an initial condition associated with the spring snowmelt and the statistical steady state mean [*Laio et al.*, 2001c]. The definition of this modified static water stress closely follows the approach presented by *Caylor et al.* [2005] who used a similar dynamic water stress measure proposed by *Porporato et al.* [2001] for the Rio Salado basin. Here we simplify the earlier approach of *Caylor et al.* [2005] and use static water stress instead in order to maintain consistency with the other examples used within this manuscript. The results presented here, however, do not change substantially between the adoption of these two measures of stress. Indeed, our suggestion is that any measure of water deficit (i.e., the duration/severity of soil moisture conditions below optimal conditions for plant growth) will provide a useful measure for delineating vegetation patterns within semiarid basins containing heterogenous vegetation, soils, and climates. We used the same approach as in the work by *Caylor et al.* [2005] to develop characteristic basin-scale profiles of plant water use ($\langle T/r \rangle$), modified static water stress ($\langle \xi' \rangle$), and stress-weighted plant water uptake normalized by average wet season rainfall, ($\langle T(1-\xi')/r \rangle$). For each variable of interest, the profile is defined as the average value of the variable (e.g., $\langle \xi'(x) \rangle$), for all points located at the same distance x from the basin outlet measured through the network [*Caylor et al.*, 2005]. Thus, in the case of the modified static water stress, the profile is determined according to

$$\langle \xi'(x) \rangle = \frac{\sum_{i=1}^{N_x} \xi'_i}{N_x}, \tag{4}$$

where N_x is the number of elementary pixels at distance x measured through the drainage network flow path, ξ'_i is modified dynamic water stress at each of these N_x locations, and $\langle\ \rangle$ notation indicates the spatial average for all points at each normalized distance x from the basin outlet ($0 \le x \le 1$). Thus, the average modified water stress profile defined in equation (4) is an average quantity conditioned on the network width function, which is itself a well-studied metric of basin geomorphology [*Marani et al.*, 1994] and is derived from analysis of USGS digital elevation data for the study basin. The same calculations are performed on plant water use, T/r and stress-weighted plant water use, $T(1-\xi')/r$ to generate basin profiles for each of these quantities.

[25] In section 2, we described how the temporal dynamics of vegetation across the Kalahari Transect act to simultaneously minimize water stress while maximizing water use. Within the topographically complex Rio Salado basin, we also find that a critical aspect of understanding basin-scale organization is the recognition that land cover patterns arise from both differential water use and differential water stress. Of particular importance is the transition between areas in the upper basin that experience large amounts of winter snowfall (effectively increasing initial growing season soil moisture availability and subsequent water use) and areas lower in the basin that experience chronic water deficit.

[26] A comparison of Figures 3a, 3b, and 3c reveals the utility of a trade-off-based optimality hypothesis that explicitly considers both resource use and resource scarcity in

Plant water use profiles

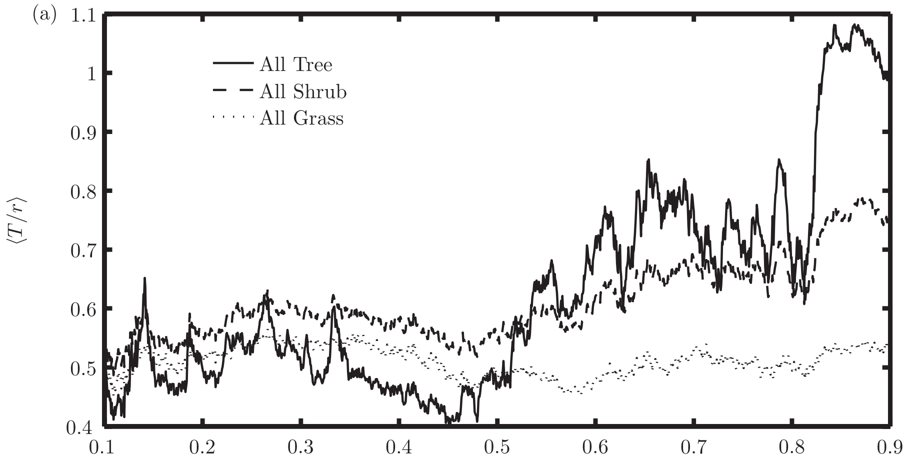

Modified plant water stress profiles

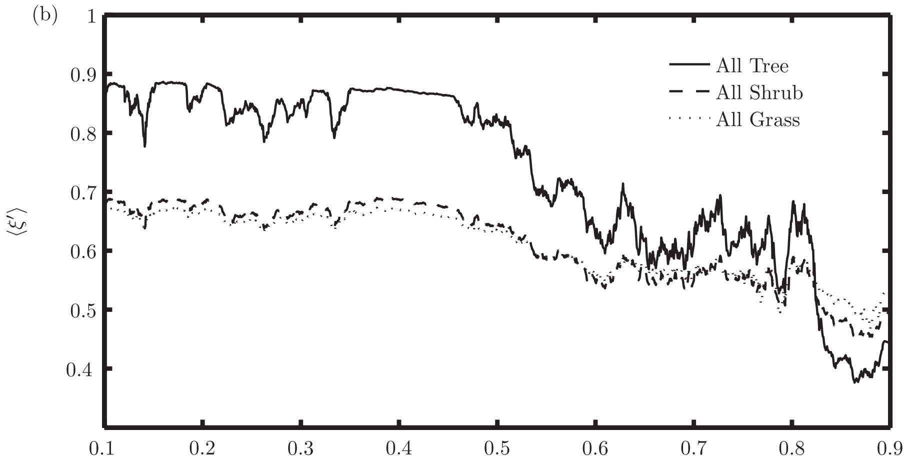

Stress-weighted plant water use profiles

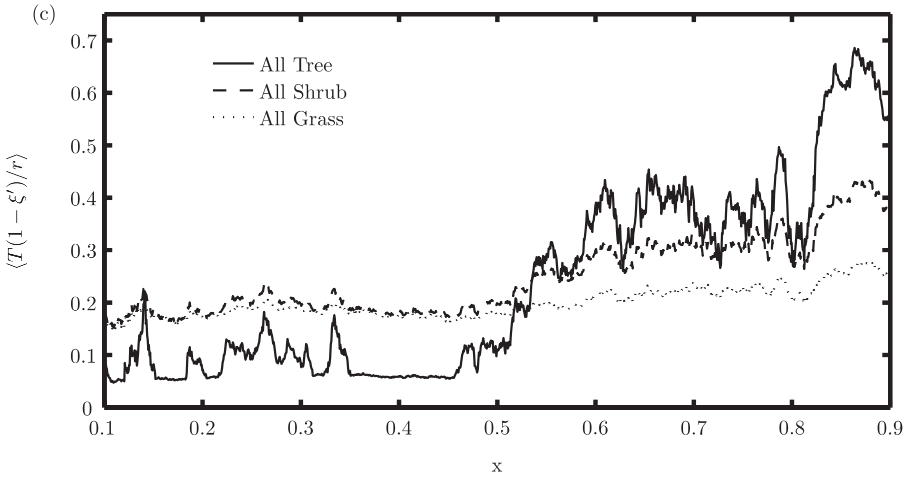

Figure 3. Profiles of (a) potential plant water use ($\langle \overline{T}/\overline{r} \rangle$), (b) modified static water stress ($\langle \overline{\xi'} \rangle$), and (c) stress-weighted plant water uptake ($\langle \overline{T}\left(1 - \overline{\xi'}\right)/\overline{r} \rangle$) for three alternative homogeneous patterns of vegetation cover within the Rio Salado basin. Angle brackets indicate a spatial average at a given normalized distance from the basin outlet as measured through basin flow paths ($0 < x < 1$), and overbars indicate a seasonal steady state average.

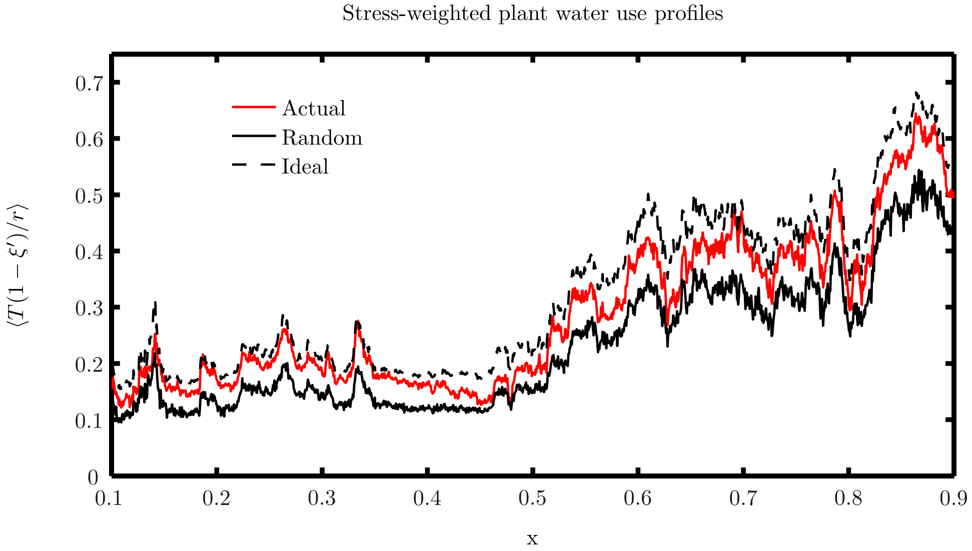

Figure 4. Three alternative profiles of stress-weighted plant water uptake. The first is the pattern that maximizes stress-weighted plant water use at each location in the basin ("ideal" pattern). The second pattern is one that corresponds to the random assignment of vegetation throughout the basin ("random" pattern), and the third represents the actual profile of stress-weighted plant water use within the basin derived from the observed pattern of land cover. The actual pattern is bounded between the random and ideal patterns but tends to more closely follow the ideal pattern across the entire profile.

the prediction of vegetation patterns within the Rio Salado basin. Each plot provides the characteristic basin profiles of plant water use (Figure 3a), modified static plant water stress (Figure 3b), and stress-weighted plant water use (Figure 3c) under three scenarios where the basin is completely vegetated by either trees, shrubs, or grasses. While Figure 3a clearly indicates that the "all tree" pattern exhibits the greatest water use in the upper portions of the basin, the ability of water use to distinguish relative performance of trees, grasses, and shrubs in the lower portions of the basin is greatly reduced. In contrast, the profiles of modified static plant water stress (Figure 3b) clearly demonstrate the higher water stress predicted for trees in the lower portion of the basin, but provide little clarification of the controls on vegetation in the upper portion of the basin, where spring snowmelt and higher rainfall lead to lower, and more similar, stress values for all three vegetation types. A comparison of the patterns of $T(1-\xi')/r$ resulting from each of these three vegetation types (Figure 3c) most closely captures the trade-offs between the importance of stress in the lower portion of the basin (which favors the presence of grasses and shrubs) and the increasing availability of water in the upper portion of the basin (which favors the presence of trees).

[27] In order to further examine the suitability of stress-weighted plant water use as a means of understanding the existing vegetation pattern of vegetation within the Rio Salado basin, we compare the actual basin-wide profile of stress-weighted plant water use (ζ) to the profiles of two alternative hypothetical vegetation distributions (Figure 4). The first is the profile of stress-weighted plant water use that arises from the specification of the vegetation type that exhibits the maximum value of stress-weighted plant water use at each location within the basin. The second hypothetical profile is the one arising from a random assignment of vegetation type at each location within the basin. In general, we find that the average stress-weighted plant water use increases at higher locations in the basin, and the spread between the maximum possible stress-weighted plant water uptake and a random stress-weighted plant water uptake ranges from 50% at the bottom of the basin to 30% at the top of the basin. We find that the stress-weighted plant water uptake that corresponds to the actual vegetation distribution lies closer to the ideal case 76% of the time. In addition, although the actual stress-weighted plant water uptake is well bounded by both the ideal and random patterns, the ideal pattern is a better overall predictor of the actual pattern than the random pattern ($R^2 = 0.90$ and $R^2 = 0.79$, respectively). Finally, the accuracy of vegetation prediction using maximum stress-weighted plant water uptake is greater than using either maximum plant water use or minimum plant water stress, which is expected given the results shown in Figure 3.

[28] Our analysis of alternative stress-weighted plant water use profiles corresponding to optimal, actual, and random vegetation patterns suggests the existence of large-scale determinants of vegetation pattern that correspond to optimality in the response to water use/water scarcity. These patterns are driven by topographic gradients in water and energy distribution within the basin, which together explain much of the variance in vegetation distribution across the basin. However, the results also indicate that a great deal of unexplained variance remains in the actual patterns of vegetation distribution observed within the basin. While our approach is not able to characterize the nature of this additional variability, it is likely that a suite of small-scale patterns will arise from local factors and ecological legacies such as those caused by dispersal, disturbance, and founder effects. Despite these smaller-scale heterogeneities, in the Rio Salado basin we observe an organization that yields an actual pattern of vegetation distribution found to lie within the envelope described by the ideal vegetation pattern that

corresponds to the maximization of stress-weighted plant water use within the basin, and a random one that preserves the overall percentage of the different types of vegetation. Having explored the landscape-scale potential for ecohydrological optimization in water-limited ecosystems, we now turn to the role of individual tree canopies on surface hydrological dynamics and their impact on patterns of vegetation structure across heterogeneous soil textures found in dryland landscapes.

4. Individual-Scale Signatures of Ecohydrological Optimization in Semiarid Landscapes

[29] While the prior two examples have been based on multiyear temporal (section 2) and large-scale spatial (section 3) patterns of land cover, it is critical to recognize that patterns of resource use, resource scarcity, and their combined impacts on vegetation are necessarily associated with the location and function of individuals. Perhaps the best known example of this approach to relating individual vegetation structure to landscape dynamic function is the paradigm of gap dynamics, by which species regeneration and subsequent patterns of canopy emergence occur within the localized patches of higher light availability formed by the death of a large canopy tree [*Shugart*, 1984]. Despite the potential utility of such approaches to address issues related to the patterns and processes operating in dryland ecosystems, there are few conceptual models that successfully relate individual structural patterns (e.g., size and distribution) to larger-scale aspects of ecosystem function (e.g., water balance).

[30] Recently, *Caylor et al.* [2006] proposed a relatively simple model of soil moisture dynamics suitable for application to structurally heterogeneous vegetation landscapes, such as those found in savannas or open woodlands. This approach was intended to provide a framework that can generate hypotheses related to the causes and effects of horizontal variation in soil moisture arising from the patchy vegetation structure of individual tree canopies that is characteristic of many semiarid ecosystems. The modeling approach is motivated by the need to characterize ecohydrological interactions between the number of co-occurring tree canopies (n_C), root systems (n_R), and their combined effect on the overall dynamics of soil moisture. Of particular interest is the manner by which the spatial pattern of both tree canopies and their accompanying root systems act to affect soil moisture dynamics. A key aspect of these above- and below-ground patterns is the lateral extent of individual root systems, and so we define the quantity $a_t = \mu_R/\mu_r$, which is specified as the ratio between the radius of a tree's root system (μ_R) and its associated canopy (μ_r). In this analysis, the value of a_t is assumed to be a fixed property of the vegetation in any landscape. Under the assumption of random tree spacing, tree centers are modeled as a two-dimensional Poisson process of rate λ_t, where λ_t represents the mean number of centers per unit area. The areal extent of each tree canopy is represented as a circle of random radius, r, drawn from an exponential distribution with mean μ_r. The areal extent of each tree's accompanying root system is represented as a circle centered on the location of the individual with radius ra_t. Thus the number, n_C, of canopies and n_R roots occurring at a randomly chosen point has a Poisson distribution [*Cox and Miller*, 1965]. In addition, the probability of finding a location in the landscape with n_R overlapping root systems and n_C overlapping canopies is the joint distribution of n_R and n_C, notated as $P(n_R \cap n_C)$.

4.1. Connecting Individual-Scale Tree Structure to Landscape-Scale Ecohydrological Optimization

[31] The joint distribution of $P(n_C \cap n_R)$ is used to connect the distribution of canopies and root systems in the landscape to the soil moisture dynamics which occur therein. We specify that the parameter n_R determines the local rate of soil water uptake, while n_C controls the evaporative loss of soil moisture and regulates the partitioning of evapotranspiration into soil evaporation and plant water uptake. The vertical root profile is here assumed to be uniform and individual plant root uptake is evenly partitioned throughout the thickness of a single soil layer, Z_r. Our data on tree active rooting depth are taken from recent field observations of dryland root distributions [*Hipondoka et al.*, 2003], which find similar vertical rooting depths across a series of sites in Botswana.

[32] We assume that canopies have a constant leaf area density, which causes a reduction in energy available for evaporation because of shading effects according to an exponential distribution (e.g., Beer's Law), and that plant water extraction rate from the soil is constrained by the total energy absorbed by individual plant canopies (cf. *Caylor et al.* [2006] for a complete model presentation). The instantaneous rates of evaporation and plant water uptake both depend on available soil moisture and potential evapotranspiration (PET, mm d^{-1}). In this approach, we assume a fixed daily PET value. Our general approach to water losses through evapotranspiration is a modified version of the scheme presented by *Laio et al.* [2001b]. In our approach, we assume that evaporation linearly increases from zero at the soil hygroscopic point, s_h, to a maximum evaporation rate, at field capacity, s_{fc}. This differs from earlier approaches [*Laio et al.*, 2001b] that assume evaporation only contributes to soil losses at soil water contents below the plant wilting point, s_w. Our formulation for plant water use is identical to that of *Laio et al.* [2001b], in that we assume that water uptake from roots (i.e., transpiration) exhibits a linear response to soil moisture availability, increasing from zero at the plant wilting point, s_w, to the maximum at the point of incipient stomatal closure, s^*. At soil moisture values above s^*, water uptake proceeds at the maximum rate, just as evaporation proceeds at the maximum rate above field capacity. Finally, above field capacity, we account for leakage loss from the lower boundary of the soil layer.

[33] At each location in a landscape containing n_C canopies and n_R roots, we consider the water stress distribution according to the frequency and magnitude of excursions of the relative soil moisture below the critical value of s^* that corresponds to the point at which plants begin to close their stomata. In order to account for the effects of increasing soil moisture deficit on plant physiological performance, we adopt the formulation of water stress (denoted as ξ) first proposed by *Rodriguez-Iturbe et al.* [1999a]. According to the hypothesis we present in this manuscript, any measure of "optimal" conditions for plant water use must appropriately balance maximization of resource use with minimization of stress occurrence. For example, as the average root

Average plant water uptake, $\langle T \rangle$ (mm/day)

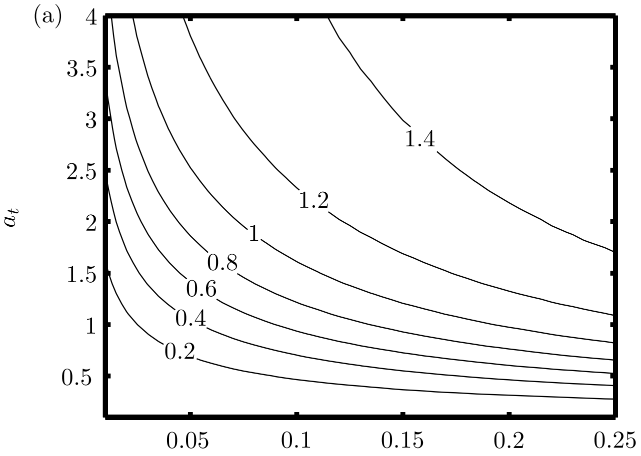

Average plant water stress, $\langle \xi \rangle$

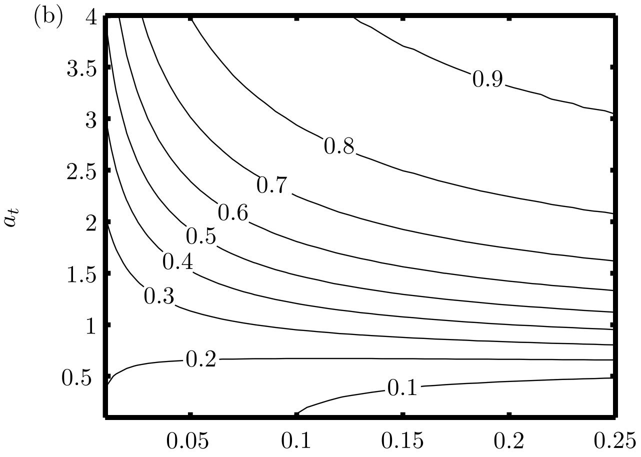

Stress-weighted plant water uptake, $\langle \zeta \rangle$ (mm/day)

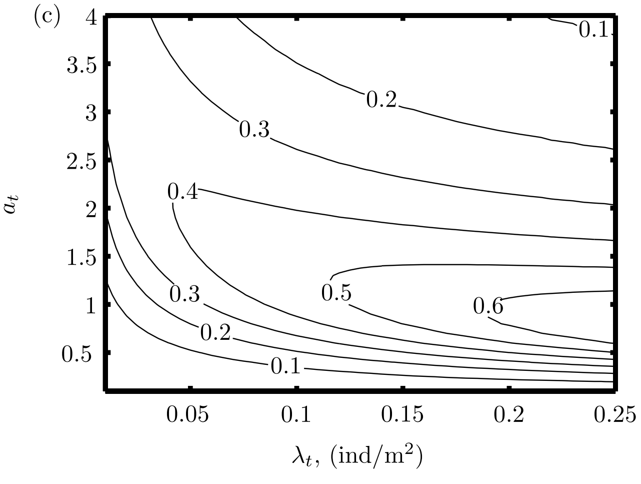

Figure 5. Effect of changing tree density, λ_t, and the ratio of lateral root radius to canopy radius, a_t, on (a) landscape average plant water uptake, $\langle T \rangle$; (b) landscape average plant water stress, $\langle \xi \rangle$; and (c) stress-weighted plant water uptake, $\langle \zeta \rangle$, for a sandy soil site with rainfall parameters of λ = 0.225 d^{-1} and α = 10 mm. Across a wide range of tree densities, there are clear optimal values of root ratios.

ratio (a_t) increases, an individual plant may be able to increase its plant water uptake rate. However, the increased number of overlapping roots associated with an increase in plant root ratio leads to higher landscape average uptake rates and more rapid onset of stress conditions whenever water becomes limiting. We adopt the approach described in section 2 to define the landscape average stress-weighted plant water uptake, $\langle \zeta \rangle$, where $\langle \; \rangle$ now represents the average stress-weighted plant water uptake within a landscape, taking into account the distribution of overlapping canopies and root zones.

[34] The local measure of plant water stress and plant water use at a location with n_C canopies and n_R root systems is combined with the joint probability of n_C and n_R to calculate the landscape average value of stress-weighted plant water uptake within landscapes of varying climates and soil types. In particular, we investigate the dependence of the landscape average stress-weighted plant water uptake on the landscape-scale vegetation structural parameters a_t and λ_t under consideration of a typical semiarid climate. The manner by which landscape average plant water use, $\langle T \rangle$, and landscape average plant water stress, $\langle \xi \rangle$, interact to determine the stress-weighted plant water uptake, $\langle \zeta \rangle$, across a range of structural configurations is depicted in Figure 5.

[35] In this example, we have chosen to use sandy soils typical of many semiarid ecosystems and a climate regime corresponding to a 6-month wet season with ~400 mm total rainfall. For these simulations, we assume a 6 mm d^{-1} potential evapotranspiration rate, and that rainfall occurs as a marked Poisson process with an average storm depth (α) of 10 mm and a rainfall occurrence rate (λ) of 0.225 storms per day, where both α and λ have exponential probability distributions. For our simulations, we have assumed that the distribution of vegetation canopies consists of exponentially distributed canopy radii with an average of 2 m corresponding to an average canopy area of 26 m^2. This specification of vegetation, climate, and soil conditions corresponds to the typical environment of the central Kalahari desert in southern Africa (cf. model description and parameter values in the work by *Caylor et al.* [2006, and references therein]). Our results demonstrate that for most conditions, increases in either tree density (λ_t) or lateral root extent (a_t) lead to corresponding increases in both average tree water use (Figure 5a) and average tree water stress (Figure 5b). In the case of plant water use, increasing root ratios (larger a_t values) always leads to higher water use, particularly at high tree densities. In the case of plant water stress, higher densities almost always lead to higher values of water stress, except for very low root ratios. For both plant water use and plant water stress, shifts in root extent have large impacts at high densities, with reduced effect of changing root ratio at low densities. Because of the manner by which both plant water use and plant water stress act to determine stress-weighted plant water uptake according to equation (3), the varying functional response of these parameters to shifts in vegetation structures means that for any tree density there exists a specific root ratio that corresponds to a local maximum of $\langle \zeta \rangle$ (Figure 5c).

4.2. Consequences of Soil Texture on Tree Structural Patterns

[36] Soil textural properties have been recognized as a factor for determining plant structural pattern in dryland

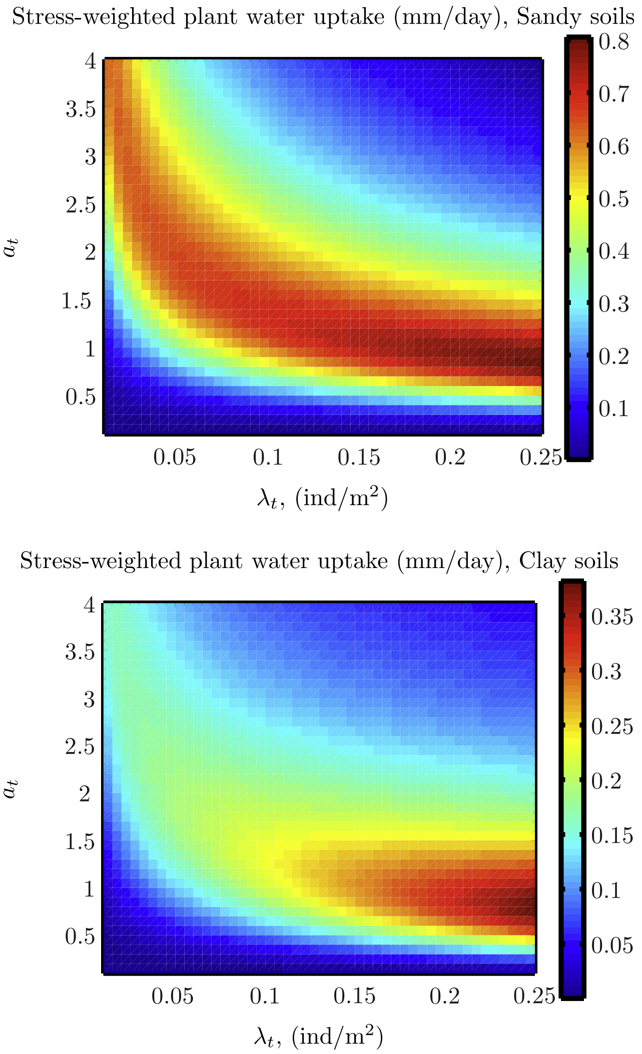
Stress-weighted plant water uptake (mm/day), Sandy soils

Stress-weighted plant water uptake (mm/day), Clay soils

Figure 6. Effect of soil texture on the amounts of stress-weighted plant water use for a typical vegetation/climate scenario (s_w = −4 MPa, s^* = −0.5 MPa). Course sandy soils allow for roughly twice the amount of stress-weighted plant water use than finely textured clay soils. Furthermore, in the case of (top) sandy soils, lower tree densities (i.e., smaller λ_t) and larger rooting areas (i.e., greater a_t) lead to only slightly reduced values of $\langle\zeta\rangle$. However, in (bottom) clay soils, similar shifts in vegetation structure lead to a much greater percentage reduction in $\langle\zeta\rangle$ values. The implication of these differences is that sandy soils can accommodate fewer, larger, and more extensively rooted species than clay soils, which provides a quantitative explanation of the inverse texture phenomenon observed in many semiarid environments.

ecosystems. In particular, many dryland ecosystems exhibit pronounced shifts in vegetation structure and composition across ecotones in soil texture. A common phenomenon is the "inverse texture effect," first described by *Noy-Meir* [1973], whereby species found in sandy soils are often larger and less drought tolerant than those found in clay soils under similar climates. The savannas of much of eastern Africa, and central Kenya in particular, provide dramatic evidence of the inverse texture effect, with large, widely spaced Acacia species dominating sandy soils adjacent to fine-textured clay soils dominated by smaller Acacia species with much higher densities. The explanation for these divergent life history strategies (large, low density in sandy soils versus small, high density in clayey soils) is an obvious challenge that any synthetic theory of ecohydrological structure and function must address.

[37] While some prior studies have shown that the presence/absence of different species on varying soil textures can be explained via differences in water balance [cf. *Fernandez-Illescas et al.*, 2001, and references therein], our focus on the explicit interactions between vegetation structure (density and lateral root extent) and function (plant water stress and plant water use) reveals pronounced shifts in optimality across soil types. In Figure 6, we demonstrate how both avoidance of water stress and maximization of water use can lead to the shifts in vegetation structure observed between sandy and clay soils. Differences in sandy/clay soils arise from changes in the saturated hydraulic conductivity, the soil porosity, and the relationship between soil water potential and volumetric water content (described with a dimensionless parameter, b, related to distribution of pore sizes within the soil). Following the values provided in Table 1 of *Laio et al.* [2001b], we use a saturated hydraulic conductivity of 220 cm d^{-1}, a porosity of 35%, and a b value of 4.05 for sandy soil. For clay soils, we adopt a saturated hydraulic conductivity of 11 cm d^{-1}, porosity of 50%, and a b value of 11.4. In both cases, we have used a fixed vegetation description, typical of savanna trees (rooting depth of 1.6 m, wilting point, s_w, of −4 MPa, an s^* value of −0.5 MPa, and an E_{max} of 5 mm d^{-1}).

[38] In terms of volumetric water content (m^3 water/m^3 soil), finer textured clay soils are capable of holding much more moisture than sandy soils. For example, in the soils used here, the same threshold tension for field capacity (−0.03 MPa) leads to a volumetric water content of 37% for the clay soils and only 13% for the sandy soil. These differences in potential water content extend to the total amount of plant available water content ($n(s_{fc} - s_w)$), which for the clay soil is 0.13 and is only 0.09 for the sandy soil. Similarly, the range of active plant water use (between s^* and s_w) is 0.05 for clay and 0.03 for the coarser sandy soil. On the basis of these differences, one might expect that clay soils would be capable of sustaining more vegetation since there is a greater potential volume of soil water within clays, and plants in clays can operate over a wider range of volumetric water contents. However, dryland soils are very rarely, if ever, at or near field capacity, and therefore it is more likely that the soils will be dry. In drying conditions, clay soils will arrive at typical semiarid plant wilting points ($\leq$−4 MPa) when the soil volumetric water content is still 25%. In contrast, sandy soils do not get to a −4 MPa wilting point threshold until only 4% volumetric water content remains. It is this difference in the lower limit of available plant water (much lower in sands) and not the total amount of potentially available plant water (slightly higher in clays) that allows for larger, lower-density trees to be found in coarser texture soils that experience the same rainfall.

[39] Figure 6 demonstrates the manner by which changes in landscape vegetation density, λ_t, and the ratio of root:canopy radius, a_t impact both the magnitude and distribution of landscape-averaged stress-weighted plant water uptake,

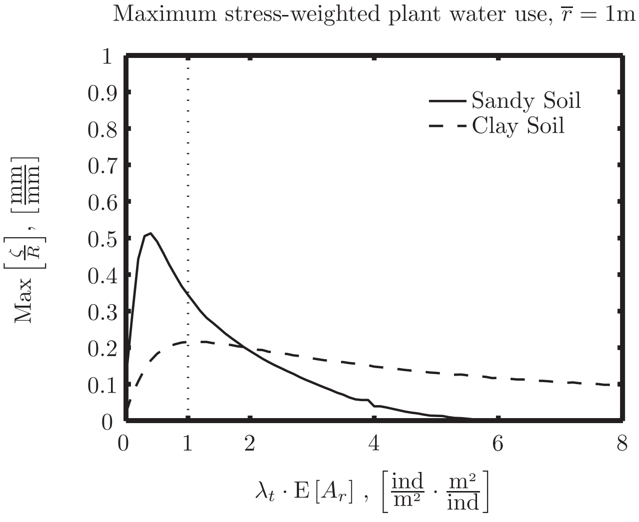

Figure 7. Effect of soil texture on the maximum stress-weighted plant water use normalized by rainfall across a range of dimensionless structural configurations. The structural axis is the product of landscape tree density, λ_t ind m^{-2}, and the expected area occupied by an individual's root system, E[A_r] (m^2 ind^{-1}), assuming that tree radii are distributed exponentially with a mean value $\overline{r} = 1$ m. Values of the dimensionless structure less than 1 indicate landscapes that have less than one individual per unit area of an individual's root zone (i.e., landscapes with unexploited soil); while values greater than 1 indicate landscapes with higher number of individuals per unit of an individual's root extent (i.e., increasing root system overlap).

$\langle\zeta\rangle$. As we observed in Figure 5c, in both sandy (Figure 6, top) and clay soils (Figure 6, bottom), the maximum value of landscape-averaged stress-weighted plant water use ($\langle\zeta\rangle$, equation (3)) occurs for high tree densities and when trees have the rooting areas close to the same size as their canopies (a_t is close to 1). However, the effect of shifting vegetation structural properties varies between the sandy and clay soil textures. In the case of sandy soils (Figure 6, top), for any specific landscape tree density, λ_t (individual trees (ind) m^{-2}), there is a corresponding lateral rooting extent, a_t, that allows for relatively constant maximum possible stress-weighted plant water use. Even at the lowest densities, high rates of stress-weighted plant water use can be maintained as long as root ratios are correspondingly large. However, in the case of clay soils, the maximum stress-weighted plant water use is not nearly as consistent across variations in tree densities and drops much faster as tree density decreases for any root ratio (Figure 6, bottom).

[40] The consistency in the maximum possible stress-weighted plant water use across a wide range of possible vegetation densities in sandy soils (Figure 6, top) implies two consequences. The first is that (using the metric we adopt here) shifts to larger, lower-density vegetation in coarse soils may not substantially alter the apparent effectiveness of the vegetation, so long as root ratios also increase as density is lowered. Secondly, there is a rather fixed relationship between changing tree density and changing tree rooting ratio in sandy soils, such that maximum stress-weighted plant water use occurs in only a narrow range of combinations of a_t and λ_t. Taken together, these results indicate that the range of structural configurations that lead to optimal conditions for vegetation growing in fine-textured soils is narrowly defined, while a greater degree of structural heterogeneity can be expected within coarsely textured soils. These results suggest that there should be lower diversity within fine-textured soils, which is indeed the case for Kenyan savannas, where a single species, *A. drepanilobium* dominates clay soils. Furthermore, *A. drepanilobium* usually occurs in dense thickets, and is characterized by a weakly developed lateral root system. Moreover, the density of *A. drepanilobium* within the areas it dominates is often greater than 3000 stems per hectare, in stark contrast to the mixed species sandy soil savannas where stem density is often an order of magnitude lower and species have much more extensive lateral root systems. It is important to note that consideration of only water use or water stress alone would not reveal these alternate structural configurations; instead, these results demonstrate that consideration of both water use and water stress is necessary to explain the divergent structure and function of savanna vegetation associated with the inverse texture effect.

[41] In general, Figure 6 seems to indicate that there are a suite of optimal relationships between tree density and rooting ratio for vegetation in coarse soils, but that for any given density, the root ratio that corresponds to the optimal value is narrowly defined (i.e., very high local gradients of $\mathrm{d}\zeta/\mathrm{d}a_t$ and $\mathrm{d}\zeta/\mathrm{d}\lambda_t$). In contrast, vegetation in finer soils seems to exhibit much greater variability in maximum stress-weighted plant water uptake, but with a less well defined optimal value for any given density (i.e., lower local gradients of $\mathrm{d}\zeta/\mathrm{d}a_t$ and $\mathrm{d}\zeta/\mathrm{d}\lambda_t$). We now explore the degree to which λ_t and a_t interact to determine maximum stress-weighted plant water use in each of these two soil types. Figure 7 depicts the maximum value of stress-weighted plant water use normalized by rainfall, $\langle T\rangle/(1 - \langle\zeta\rangle)/r$, across a single nondimensional measure of plant structure. We determine this structural measure as the product of plant density (λ_t, ind m^{-2}) and the average area of an individual's rooting zone, E[A_r] (m^2 ind^{-1}). The specific value of E[A_r] depends on two parameters: the rooting ratio, a_t, and the average canopy size, characterized by the mean canopy radius, $\overline{r}$ (m). Assuming that r is a random variable, the value of E[A_r] also depends on the underlying probability distribution of individual canopy radii sizes. Here we assume that the values of r within the landscape are exponentially distributed, so that

$$\mathrm{E}[A_r] = 2\pi(\overline{r} \cdot a_t)^2. \tag{5}$$

[42] Viewed from the perspective of a composite nondimensional structure (number of individuals in an average individual's root area), the differences between coarse- and fine-textured soils appears differently (Figure 7). Once again, the ability of sandy soils to have a higher maximum possible stress-weighted water use is apparent, but now it is more obvious that the density and root areas of vegetation in sandy soils must lie in a narrow range of combinations, so that the number of individuals per unit individual root area is always close to 0.5. Because the expected area of individual root areas is twice the area of the rooting area

of an average-sized individual when individual sizes are exponentially distributed (equation (5)), the implication is that individuals in a sandy soil will rarely have any rooting overlap if stress-weighted plant water use is to be optimized. In contrast, the rather slow reduction in maximum possible stress-weighted plant water uptake in fine-textured soils suggests that the degree of root overlap in these soils can be quite high and still achieve relatively high levels of stress-weighted plant water use. Once again, these results point to a fundamental distinction between dryland vegetation experiencing similar rainfall amounts, but varying soil textures: vegetation within sandy soils should be more widely spaced at any density, with substantially less lateral overlap of rooting zones than vegetation in finer-textured clayey soils, where substantial rooting overlap may occur.

5. Conclusion

[43] This article has briefly reviewed three efforts to describe ecohydrological trade-offs that lead to organization of vegetation patterns in water-limited landscapes. In each case, we have examined a different scale of interest, from regional to individual, through a suite of numerical and analytical modeling approaches. The essence of a trade-off-based approach to understanding vegetation function has long been inherent to coupled models of carbon and water dynamics [*Guswa*, 2008; *Schymanski et al.*, 2008a, 2008b; *van der Tol et al.*, 2008a, 2008b], which usually relate water stress to stomatal closure and thus are able to compute the direct effect of stomatal conductance on the carbon uptake rate. However, we believe there remain substantial advantages to approaches that seek to characterize plant patterns and dynamics solely through the prism of surface water balance. Most critically, models that consider a trade-off that includes optimization of carbon uptake introduce a nonconservative quantity into the optimization framework. In contrast, our approach considers only the use and availability of a resource that is completely conservative within the system we are examining, so our objective function is always bounded by upper and lower limits that have physical meaning. For instance, assuming rainfall is the only source of soil water, our stress weighted plant water uptake function is always limited at the upper bound by total rainfall amounts at seasonal to annual time scales. Therefore, in our view, an approach that considers carbon/water trade-offs benefits from a more mechanistic understanding of how resource scarcity impacts plant function but at the expense of an unbounded objective function that makes comparisons between sites or across gradients of resource availability much more difficult.

[44] While we believe the trade-off-based approach we have presented here has some distinct advantages in terms of its generality and explicit focus on conservative quantities, the application of our framework to quantitative predictions relies on quantitative measures of both resource use as well as the effects of resource scarcity. In terms of resource use, the tight couplings between plant transpiration and plant carbon uptake make it possible to relate water use to growth at a range of spatial and temporal scales, from individual leaves to entire ecosystems. However, it remains difficult to separate the direct effects of water stress on plants independent of the indirect effects of water scarcity on growth. Research regarding the effect of soil water deficits on xylem cavitation and plant hydraulic conductivity may lead to novel and more generalized approaches for inferring the impact of water scarcity on whole plant function. In the absence of a quantitative means for assessing stress and growth independently, clear distinctions between our trade-off-based hypotheses and those that seek to maximize growth will remain difficult to define. However, as ecohydrological research proceeds to develop a clearer understanding of the functional impacts of resource scarcity, water stress itself will likely become a more quantitative measure of plant status. In this case, we expect that a trade-off-based approach of the type that we have described here will yield substantially improved predictions regarding the dynamics of savanna ecosystem structure, and the coexistence of alternate strategies for dealing with the chronic intermittent water availability that exemplifies dryland ecosystems.

[45] Here we have used a series of related but independent examples to demonstrate the utility of a unified approach based only on the water balance and resulting measures of plant water deficit/use as a diagnostic tool for assessing optimality of plant structural pattern. In particular, we find that a trade-off function that describes a stress-weighted plant water use provides substantial insight into spatial and temporal patterns of vegetation in all three examples. Clearly, such modeling approaches will continue to generate hypotheses at a much greater rate than they are able to confirm them. However, it is our hope that the ongoing development of coupled ecological and hydrological models capable of assessing a diversity of interactions between plants, soils, and climates will lead to the emergence of more generalized hypotheses regarding the manner by which ecological and hydrological patterns coorganize in landscapes. The results presented here suggest that greatest insight into the determinants of ecohydrological patterns and processes may lie in methods that seek to describe vegetation structure and function according to consideration of explicit trade-offs that occur between the dual necessities of resource consumption and the avoidance of resource scarcity.

[46] **Acknowledgments.** K.K.C. and T.M.S. acknowledge the support of NASA's Interdisciplinary Science Program (NASA-NNG-04-GM71G). K.K.C. also acknowledges the support of the NSF through grants DEB-742933 and EAR-0847368. I.R.-I. acknowledges the support of NSF through grant EAR-0642550. A key preliminary version of this manuscript was presented by the authors at the meeting on Water and the Environment. The proceedings of that meeting were published by the Vatican Academy of Sciences in 2008. The authors are extremely grateful to Associate Editor Drew Guswa, Stan Schmanski, and two anonymous reviewers for their extremely helpful and insightful comments on an earlier version of this manuscript.

References

Albertson, J. D., and N. Montaldo (2003), Temporal dynamics of soil moisture variability: 1. Theoretical basis, *Water Resour. Res.*, *39*(10), 1274, doi:10.1029/2002WR001616.

Bond, B. J. (2003), Hydrology and ecology meet—And the meeting is good, *Hydrol. Processes*, *17*, 2087–2089.

Bond, W. J., G. F. Midgley, and F. I. Woodward (2003), The importance of low atmospheric CO_2 and fire in promoting the spread of grasslands and savannas, *Global Change Biol.*, *9*(7), 973–982.

Breshears, D. D. (2005), An ecologist's perspective of ecohydrology, *Bull. Ecol. Soc. Am.*, *86*(4), 296–300.

Breshears, D. D., et al. (2005), Regional vegetation die-off in response to global-change-type drought, *Proc. Natl. Acad. Sci. U. S. A.*, *102*(42), 15,144–15,148.

Brown, J. R., and S. Archer (1999), Shrub invasion of grassland: Recruitment is continuous and not regulated by herbaceous biomass or density, *Ecology*, *80*(7), 2385–2396.

Caylor, K. K., P. R. Dowty, H. H. Shugart, and S. Ringrose (2004a), Relationship between small-scale structural variability and simulated vegetation productivity across a regional moisture gradient in southern Africa, *Global Change Biol.*, *10*(3), 374–382.

Caylor, K. K., T. M. Scanlon, and I. Rodriguez-Iturbe (2004b), Feasible optimality of vegetation patterns in river basins, *Geophys. Res. Lett.*, *31*, L13502, doi:10.1029/2004GL020260.

Caylor, K. K., S. Manfreda, and I. Rodriguez-Iturbe (2005), On the coupled geomorphological and ecohydrological organization of river basins, *Adv. Water Resour.*, *28*(1), 69–86.

Caylor, K. K., P. D'Odorico, and I. Rodriguez-Iturbe (2006), On the ecohydrology of structurally heterogeneous semiarid landscapes, *Water Resour. Res.*, *42*, W07424, doi:10.1029/2005WR004683.

Cox, D., and H. Miller (1965), *The Theory of Stochastic Processes*, Methuen, London.

Daly, C., D. Bachelet, J. M. Lenihan, R. P. Neilson, W. Parton, and D. Ojima (2000), Dynamic simulation of tree-grass interactions for global change studies, *Ecol. Appl.*, *10*(2), 449–469.

Eagleson, P. S. (1978), Climate, soil and vegetation: 1. A simplified model of soil moisture movement in the liquid phase, *Water Resour. Res.*, *14*(5), 722–730.

Eagleson, P. S. (2002), *Ecohydrology: Darwinian Expression of Vegetation Form and Function*, Cambridge Univ. Press, Cambridge, U. K.

Eagleson, P. S., and R. I. Segarra (1985), Water-limited equilibrium of savanna vegetation systems, *Water Resour. Res.*, *21*(10), 1483–1493.

Edreny, T. A. (2005), Ecohydrology: A synthesis of Newtonian and Darwinian world views, *Hydrol. Processes*, *19*, 2315–2317.

Feddes, R. A., P. Kabat, P. J. T. Van Bakel, J. J. B. Bronswijk, and J. Halbertsma (1988), Modelling soil water dynamics in the unsaturated zone—State of the art, *J. Hydrol.*, *100*(1–3), 69–111.

Fernandez-Illescas, C. P., A. Porporato, F. Laio, and I. Rodriguez-Iturbe (2001), The ecohydrological role of soil texture in a water-limited ecosystem, *Water Resour. Res.*, *37*(12), 2863–2872.

Goward, S. N., and S. D. Prince (1995), Transient effects of climate on vegetation dynamics: Satellite observations, *J. Biogeogr.*, *22*(2–3), 549–564.

Guenther, A., L. Otter, P. Zimmerman, J. Greenberg, R. Scholes, and M. Scholes (1996), Biogenic hydrocarbon emissions from southern African savannas, *J. Geophys. Res.*, *101*(D20), 25,859–25,865.

Guswa, A. J. (2008), The influence of climate on root depth: A carbon cost-benefit analysis, *Water Resour. Res.*, *44*, W02427, doi:10.1029/2007WR006384.

Hannah, D. M., P. J. Wood, and J. P. Sadler (2004), Ecohydrology and hydroecology: A new paradigm'?, *Hydrol. Processes*, *18*, 3439–3445, doi:10.1002/hyp.5761.

Hatton, T. J., G. D. Salvucci, and H. I. Wu (1997), Eagleson's optimality theory of an ecohydrological equilibrium: Quo vadis?, *Funct. Ecol.*, *11*, 665–674.

Hipondoka, M. H., J. N. Aranibar, C. Chirara, M. Lihava, and S. A. Macko (2003), Vertical distribution of grass and tree roots in arid ecosystems of southern Africa: Niche differentiation or competition?, *J. Arid Environ.*, *54*(2), 319–325.

Huxman, T. E., B. P. Wilcox, D. D. Breshears, R. L. Scott, K. A. Snyder, E. E. Small, K. Hultine, W. T. Pockman, and R. B. Jackson (2005), Ecohydrological implications of woody plant encroachment, *Ecology*, *86*(2), 308–319.

Jeltsch, F., K. Moloney, and S. J. Milton (1999), Detecting process from snapshot pattern: Lessons from tree spacing in the southern Kalahari, *Oikos*, *85*(3), 451–466.

Jeltsch, F., G. E. Weber, and V. Grimm (2000), Ecological buffering mechanisms in savannas: A unifying theory of long-term tree-grass coexistence, *Plant Ecol.*, *150*(1–2), 161–171.

Kerkhoff, A. J., S. N. Martens, and B. T. Milne (2004), An ecological evaluation of Eagleson's optimality hypotheses, *Funct. Ecol.*, *18*, 404–413.

Koch, G. W., P. M. Vitousek, W. L. Steffen, and B. H. Walker (1995), Terrestrial transects for global change research, *Vegetatio*, *121*, 53–65.

Laio, F., A. Porporato, C. P. Fernandez-Illescas, and I. Rodriguez-Iturbe (2001a), Plants in water-controlled ecosystems: Active role in hydrologic processes and response to water stress—IV. Discussion of real cases, *Adv. Water Resour.*, *24*(7), 745–762.

Laio, F., A. Porporato, L. Ridolfi, and I. Rodriguez-Iturbe (2001b), Plants in water-controlled ecosystems: Active role in hydrologic processes and response to water stress—II. Probabilistic soil moisture dynamics, *Adv. Water Resour.*, *24*(7), 707–723.

Laio, F., A. Porporato, L. Ridolfi, and I. Rodriguez-Iturbe (2001c), Mean first passage times of processes driven by white shot noise, *Phys. Rev. E*, *63*, 036105, doi:10.1103/PhysRevE.63.036105.

Levin, S. A. (1999), *Fragile Dominion: Complexity and the Commons*, Perseus Books, Reading, Mass.

Ludwig, J. A., B. P. Wilcox, D. D. Breshears, D. J. Tongway, and A. C. Imeson (2005), Vegetation patches and runoff-erosion as interacting ecohydrological processes in semiarid landscapes, *Ecology*, *86*(2), 288–297.

Marani, M., A. Rinaldo, R. Rigon, and I. Rodriguez-Iturbe (1994), Geomorphological width functions and the random cascade, *Geophys. Res. Lett.*, *21*(19), 2123–2126.

Newman, B. D., B. P. Wilcox, S. R. Archer, D. D. Breshears, C. N. Dahm, C. J. Duffy, N. G. McDowell, F. M. Phillips, B. R. Scanlon, and E. R. Vivoni (2006), Ecohydrology of water-limited environments: A scientific vision, *Water Resour. Res.*, *42*, W06302, doi:10.1029/2005WR004141.

Noy-Meir, I. (1973), Desert ecosystems: Environment and predators, *Annu. Rev. Ecol. Syst.*, *4*, 25–51.

Porporato, A., F. Laio, L. Ridolfi, and I. Rodriguez-Iturbe (2001), Plants in water-controlled ecosystems: Active role in hydrologic processes and response to water stress—III. Vegetation water stress, *Adv. Water Resour.*, *24(7), 725–744.*

Privette, J. L., Y. Tian, G. Roberts, R. J. Scholes, Y. Wang, K. K. Caylor, P. Frost, and M. Mukelabai (2004), Vegetation structure characteristics and relationships of Kalahari woodlands and savannas, *Global Change Biol.*, *10*(3), 281–291.

Rodriguez-Iturbe, I., and A. Porporato (2004), *Ecohydrology of Water-Controlled Ecosystems*, Cambridge Univ. Press, Cambridge, U. K.

Rodriguez-Iturbe, I., P. D'Odorico, A. Porporato, and L. Ridolfi (1999a), On the spatial and temporal links between vegetation, climate, and soil moisture, *Water Resour. Res.*, *35*(12), 3709–3722.

Rodriguez-Iturbe, I., A. Porporato, L. Ridolfi, V. Isham, and D. R. Cox (1999b), Probabilistic modelling of water balance at a point: The role of climate, soil and vegetation, *Proc. R. Soc. London, Ser. A*, *455*, 3789–3805.

Rodriguez-Iturbe, I., A. Porporato, F. Laio, and L. Ridolfi (2001), Plants in water-controlled ecosystems: Active role in hydrologic processes and response to water stress—I. Scope and general outline, *Adv. Water Resour.*, *24*(7), 695–705.

Sankaran, M., et al. (2005), Determinants of woody cover in African savannas, *Nature*, *438*, 846–849.

Scanlon, T. M., and J. D. Albertson (2003), Inferred controls on tree/grass composition in a savanna ecosystem: Combining 16-year normalized difference vegetation index data with a dynamic soil moisture model, *Water Resour. Res.*, *39*(8), 1224, doi:10.1029/2002WR001881.

Scanlon, T. M., and J. D. Albertson (2004), Canopy scale measurements of CO_2 and water vapor exchange along a precipitation gradient in southern Africa, *Global Change Biol.*, *10*(3), 329–341.

Scanlon, T. M., J. D. Albertson, K. K. Caylor, and C. Williams (2002), Determining land surface fractional cover from NDVI and rainfall time series for a savanna ecosystem, *Remote Sens. Environ.*, *82*(2–3), 376–388.

Scanlon, T. M., K. K. Caylor, S. Manfreda, S. A. Levin, and I. Rodriguez-Iturbe (2005), Dynamic response of grass cover to rainfall variability: Implications for the function and persistence of savanna ecosystems, *Adv. Water Resour.*, *28*(3), 291–302.

Scanlon, T. M., K. K. Caylor, I. Rodriguez-Iturbe, and S. A. Levin (2007), Positive feedbacks promote power-law clustering of Kalahari vegetation, *Nature*, *449*, 209–212, doi:10.1038/nature06060.

Scholes, R. J., and B. H. Walker (1993), *An African Savanna: Synthesis of the Nylsvley Study*, Cambridge Univ. Press, Cambridge, U. K.

Scholes, R. J., P. R. Dowty, K. K. Caylor, D. A. B. Parsons, P. G. H. Frost, and H. H. Shugart (2002), Trends in savanna structure and composition on an aridity gradient in the Kalahari, *J. Vegetation Sci.*, *13*(3), 419–428.

Schwinning, S., and J. R. Ehleringer (2001), Water use trade-offs and optimal adaptations to pulse-driven arid ecosystems, *J. Ecol.*, *89*(3), 464–480.

Schymanski, S. J., M. L. Roderick, M. Sivapalan, L. B. Hutley, and J. Beringer (2008a), A canopy-scale test of the optimal water-use hypothesis, *Plant Cell Environ.*, *31*(1), 97–111.

Schymanski, S. J., M. Sivapalan, M. L. Roderick, J. Beringer, and L. B. Hutley (2008b), An optimality-based model of the coupled soil moisture and root dynamics, *Hydrol. Earth Syst. Sci. Discuss.*, *5*, 51–94.

Seyfried, M. S., S. Schwinning, M. A. Walvoord, W. T. Pockman, B. D. Newman, R. B. Jackson, and F. M. Phillips (2005), Ecohydrological control of deep drainage in arid and semiarid regions, *Ecology*, *86*(2), 277 – 287.

Shugart, H. H. (1984), *A Theory of Forest Dynamics*, Springer, New York.

Smit, G. N., and N. F. G. Rethman (2000), The influence of tree thinning on the soil water in a semi-arid savanna of southern Africa, *J. Arid Environ.*, *44*, 41 – 59.

Sole, R. V. (2007), Scaling laws in the drier, *Nature*, *449*, 151 – 153, doi:10.1038/449151a.

Thomas, D. S. G., and P. A. Shaw (1991), *The Kalahari Environment*, Cambridge Univ. Press, Cambridge, U. K.

van der Tol, C., A. J. Dolman, M. J. Waterloo, and G. C. A. A.Meesters (2008a), Optimum vegetation characteristics, assimilation, and transpiration during a dry season: 2. Model evaluation, *Water Resour. Res.*, *44*, W03422, doi:10.1029/2007WR006243.

van der Tol, C., A. G. C. A. Meesters, A. J. Dolman, and M. J. Waterloo (2008b), Optimum vegetation characteristics, assimilation, and transpiration during a dry season: 1. Model description, *Water Resour. Res.*, *44*, W03421, doi:10.1029/2007WR006241.

Williams, C. A., and J. D. Albertson (2005), Contrasting short- and long-timescale effects of vegetation dynamics on water and carbon fluxes in water-limited ecosystems, *Water Resour. Res.*, *41*, W06005, doi:10.1029/2004WR003750.

K. K. Caylor and I. Rodriguez-Iturbe, Department of Civil and Environmental Engineering, Engineering Quadrangle, Princeton University, Princeton, NJ 08544, USA. (kcaylor@princeton.edu)

T. M. Scanlon, Department of Environmental Sciences, University of Virginia, Charlottesville, VA 22904, USA.